Journal of Pharmaceutical Analysis 12 (2022) 96–103

Contents lists available at ScienceDirect

Journal of Pharmaceutical Analysis

journal homepage: www.elsevier.com/locate/jpa

Original article

# Fabrication of edge-curled petals-like covalent organic frameworks and their properties for extracting indole alkaloids from complex biological samples

Fanrong Sun [a, b], Ligai Bai [a, b, c, *], Mingxue Li [a, b], Changqing Yu [a, b], Haiyan Liu [a, b, c], Xiaoqiang Qiao [a, b, c], Hongyuan Yan [a, b, c, **]

[a] College of Pharmaceutical Sciences, Hebei University, Baoding, 071002, Hebei, China
[b] Key Laboratory of Medicinal Chemistry and Molecular Diagnosis of Ministry of Education, Baoding, 071002, Hebei, China
[c] Institute of Life Science and Green Development, Hebei University, Baoding, 071002, Hebei, China

ARTICLE INFO

*Article history:*
Received 12 June 2020
Received in revised form
17 September 2020
Accepted 20 December 2020
Available online 24 December 2020

*Keywords:*
Covalent organic frameworks
Monolithic material
Solid-phase extraction
Alkaloids
Biological samples

ABSTRACT

In this study, a functionalized covalent-organic framework (COF) was first synthesized using porphyrin as the fabrication unit and showed an edge-curled, petal-like and well-ordered structure. The synthesized COF was then introduced to prepare porous organic polymer monolithic materials (POPMs). Two composite POPM/COF monolithic materials with rod shapes, referred to as sorbent A and sorbent B, were prepared in stainless steel tubes using different monomers. Sorbents A and B exhibited relatively uniform porous structures and enhanced specific surface areas of 153.14 $m^2/g$ and 80.01 $m^2/g$, respectively. The prepared composite monoliths were used as in-tube solid-phase extraction (SPE) sorbents combined with HPLC for the on-line extraction and quantitative analytical systems. Indole alkaloids (from *Catharanthus roseus* G. Don and *Uncaria rhynchophylla* (Miq.) Miq. Ex Havil.) contained in mouse plasma were extracted and quantitatively analyzed using the online system. The two composite multifunctional monoliths showed excellent clean-up ability for complex biological matrices, as well as superior selectivity for target indole alkaloids. Method validation showed that the RSD values of the repeatability ($n$=6) were $\leq$ 3.46%, and the accuracy expressed by the spiked recoveries was in the ranges of 99.38%–100.91% and 96.39%–103.50% for vinca alkaloids and *Uncaria* alkaloids, respectively. Furthermore, sorbents A and B exhibited strong reusability, with RSD values $\leq$ 5.32%, which were based on the peak area of the corresponding alkaloids with more than 100 injections. These results indicate that the composite POPM/COF rod-shaped monoliths are promising media as SPE sorbents for extracting trace compounds in complex biological samples.



## 1. Introduction

Covalent organic frameworks (COFs) have rigid construction units constructed by the first and second cycles of lighter elements, such as H, B, C, N, and O, through covalent bond connections [1]. These COFs exhibit the fascinating features of permanent porosity, tunable pore size, large specific surface area, and excellent resistance to heat and hydrolysis [2,3]. The Schiff base reaction based on imine requires mild conditions and is catalyst free, and the generated COFs have better structure regularity and order, which confers stability in most organic solvents [4–6]. Furthermore, COFs have demonstrated unique advantages in the adsorption and separation fields [7–12]. Porous organic polymer-based, rod-shaped materials (POPMs) have extensive material selection, simple preparation, good permeability, and an adjustable pore structure and can easily achieve multifunctional modification, all of which result in proper solid-phase extraction (SPE) sorbents [13–15]. However, the shortcoming in spite of the multiple advantages is

Peer review under responsibility of Xi'an Jiaotong University.
* Corresponding author. College of Pharmaceutical Sciences, Hebei University, Baoding, 071002, Hebei, China.
** Corresponding author. College of Pharmaceutical Sciences, Hebei University, Baoding, 071002, Hebei, China.
*E-mail addresses:* bailigai@163.com (L. Bai), yanhongyuan@126.com (H. Yan).

https://doi.org/10.1016/j.jpha.2020.12.006

that the specific surface area of POPMs is relatively small due to the macropore structure, which makes it difficult to have rich action sites and multiple action mechanisms to satisfy the extraction and separation of multiactive components in complex samples [16,17]. Therefore, it is necessary to introduce a material with a large specific surface area to improve the POPM's specific surface area. Combining the advantages of POPMs and COFs is a feasible method to enhance the surface area of POPMs and to enrich the interactions. Based on the in-built covalent bond structure, COFs are anticipated to be more suitable scaffolds to combine with POPMs than other porous materials; thus, POPMs/COFs will emerge as efficient and versatile SPE sorbents. The properties of an SPE sorbent are the most important factors affecting the selectivity, extraction efficiency, and accuracy of the analysis result [18]. The materials commonly used as SPE sorbents are chemically bonded silica-based materials [19], carbon-based materials [20] and polymer-based materials [21]. Many new materials have been used as SPE sorbents in recent years to compensate for the narrow pH range, low adsorption capacity and low reuse rate of the original sorbents. Some of the materials include molecularly imprinted polymers (MIPs) [22], magnetic nanoparticles (MNPs) [23], carbon nanotubes (CNTs) [24], graphene/graphene oxide (G/GO) [25], metallic and metal oxide nanoparticles [26], metal organic frameworks (MOFs) [27,28], and COFs [29]. Although all these materials have special advantages, they usually have a single adsorption mechanism, which is only selected for a certain type of component, is unable to distinguish components with similar structures and natures, and cannot avoid the non-selective adsorption of biological matrix. The result of this narrow selection is competitive adsorption between the matrix and active components, which seriously affects the extraction efficiency and the accuracy of analysis results. The selectivity of the SPE method for the target components not only depends on the interaction between the target components and the sorbent but is also seriously influenced by the interaction between the matrix and the sorbent [30,31]. As a result, an excellent SPE sorbent should be fabricated to aim at both the sample matrix and the target component, have a relatively high specific surface area, have multi-functional chemical groups, and have multi-dimensional pores; thus, the matrix and the target component will take their place due to different interactions and different molecular kinetic diameters.

Complex samples, including herbal extracts and mouse blood, are difficult to analyze because of their complex matrices and low-concentration targets and usually require pre-treatment before separation and analysis [32,33]. Compared to protein precipitation and liquid-liquid extraction, SPE, as it requires less solvent, has a relatively higher extraction efficiency and can be easily performed in automatic ways, which makes SPE an effective method for the pre-treatment and separation of trace components from complex samples [34,35]. The SPE modes mainly include cartridges, disks, pipette tips, multiwell plates and dispersive SPE, among which cartridges are the most frequently chosen in the field of pre-treating complex samples. Concurrently, cartridges are the most commercially available and used configuration of SPE and make on-line SPE procedures easy to establish [36,37]. However, commercial cartridges, including $C_{18}$ guard columns, are usually single-use materials, which increases the cost of analysis.

In the present work, a porphyrin-based COF functionalized with a double bond was synthesized via a solvothermal synthesis method. The resulting COF exhibited an edge-curled, petal-like and well-ordered structure. Two composite rod-shaped POPM/COF-SPE sorbents were prepared in 50-mm long stainless steel tubes with inner diameter of 4.6 mm, and SPE-HPLC systems were constructed for online extraction, enrichment and quantitative analysis of indole alkaloids contained in plants and mouse plasma. The chemical structures of the indole alkaloids are shown in Fig. S1.

## 2. Experimental

### 2.1. Materials

Diallyl maleate (DAM), methacrylic anhydride (MA), o-dichlorobenzene, N,N-dimethyl aniline (DMA), tetrahydrofurfuryl methacrylate (THFMA) and triethylamine were purchased from Aladdin Reagent Co., Ltd. (Shanghai, China). HPLC grade methanol (MeOH), HPLC grade acetonitrile (ACN), n-propanol, n-butanol, polyethylene glycol 200, isocyanuric acid triallyl ester (TAIC) and tetrahydrofuran (THF) were purchased from Kermel Chemical Reagent Factory (Tianjin, China). Ethylene glycol dimethacrylate (EDMA) was purchased from Shanghai Macklin Biochemical Co., Ltd. (Shanghai, China). 1-Dodecanol, ethyl acetate, acetic acid, absolute ethyl alcohol, phosphoric acid and benzoyl peroxide (BPO) were obtained from Tianjin Guangfu Technology Development Co., Ltd. (Tianjin, China). The alkaloid reference standards were purchased from Beijing Century Aoko Biotechnology Co., Ltd. (Beijing, China). 5,10,15,20-Tetrakis (4-hydroxyphenyl)porphyrin (Tph) and 2,4,6-triformylphloroglucinol (Tp) were supplied by Tokyo Chemical Industry Co., Ltd. (Tokyo, Japan). *Catharanthus roseus* G. Don (*C. roseus*) and *Uncaria rhynchophylla* (Miq.) Miq. Ex Havil. (*Uncaria*) were purchased from TongRenTang Co., Ltd. (Beijing, China). An Agilent ZORBAX Eclipse Plus $C_{18}$ column (150 mm × 4.6 mm i.d., 5 μm, Agilent Technologies, Inc., Santa Clara, CA, USA) and COSMOSIL $C_{18}$ column (250 mm × 4.6 mm i.d., 5 μm, Nakarai Tesque, Inc., Kyoto, Japan) were used.

The water used in all experiments was ultrapure water. The mobile phase and samples were filtered through a microfiltration membrane with pore diameters of 0.45 and 0.22 μm, respectively.

### 2.2. Instruments

The morphology of the prepared materials was determined using a Phenom-World BV scanning electron microscope (SEM) (Eindhoven, the Netherlands). The infrared (IR) spectra were assayed on a Shimaduzu Fourier transform infrared spectroscopy (FTIR)-8400S Spectrometer (Tokyo, Japan). The PXRD pattern was determined on an X-ray powder diffractometer (Bruker Technology Co., Ltd., Karlsruhe, Germany). Nitrogen adsorption/desorption analysis was measured using a TriStar II 3020 automatic surface area and porosity analyser (Micromeritics Instrument Corporation, Norcross, GA, USA). Chromatographic experiments were performed on an LC-3000 HPLC instrument (Beijing Hengke Innovation Technology Co., Ltd., Beijing, China) with a UV detector and a data acquisition workstation. Ultrapure water was produced by an ultrapure water instrument (UPT–II–5T, Sichuan Ultrapure Technology Co., Ltd., Chengdu, China).

The preparation of the sample and solution is shown in the Supplementary data file.

### 2.3. Synthesis of the COF

MA (0.1863 g), Tp (0.021 g) and THF (20 mL) were mixed in a flask and stirred at 60 °C for 48 h. When the reaction finished, THF was removed using a rotary evaporator at 60 °C. The precipitate in the flask was dissolved in 20 mL of ethyl acetate and subsequently washed three times with 10 mL of water. This process produced a yellow liquid product. The ethyl acetate containing the solute was

placed in an evaporating dish at −20 °C overnight and then freeze-dried to obtain the Tp-MA product. The obtained Tp-MA (0.0207 g) and Tph (0.0337 g) were dissolved in 10 mL of absolute ethyl alcohol prior to dissolving in a mixture of acetic acid (2 mL, 6 mol/L), o-dichlorobenzene (10 mL) and absolute ethyl alcohol (10 mL). The solution was refluxed for 72 h at 120 °C and then centrifuged for 10 min with centrifugal force of 1,200 *g*. Finally, the product, which was referred to as TpTph-MA-COF, was obtained when the precipitate was cooled and dried [38–40]. Scheme 1 shows the reactive processes.

### 2.4. Preparation of monolithic POPM/COF-SPE sorbents

TpTph-MA-COF and DAM were used as co-monomers, EDMA as the crosslinker, and n-propanol and dodecanol as porogens. These reactants were poured into a 50-mm-long stainless steel chromatographic tube with a 4.6-mm inner diameter and allowed to polymerize at 30 °C for 3 h initiated by BPO/DMA. The completely polymerized rod-shaped monolithic sorbent, referred to as sorbent A, was washed online with MeOH using an HPLC system to remove the porogenic solvents. Sorbent B was prepared using TpTph-MA-COF and THFMA as the co-monomers, TAIC and EDMA as the co-crosslinkers, as well as DMF, n-propanol and dodecanol as porogens, via the same procedure as that of sorbent A. The synthetic processes are shown in Fig. S2, and the representative compositions of the preparative pre-polymerization solution are shown in Table 1.

### 2.5. SPE-HPLC procedure

As shown in Fig. S3, the two kinds of rod-shaped sorbents were installed at the sample loop of the six-way valve, thus building an online SPE-HPLC system in conjunction with an HPLC system using a $C_{18}$ column. *C. roseus* and mouse plasma containing multiple alkaloids were used as the samples for testing sorbents A and B, respectively. Removal of the sample matrices and simultaneous extraction of the target alkaloids were implemented using a "column switch" method, and the procedures were as follows: sample matrices were washed using proper eluent when the six-way valve was at the "Load" position, and subsequently, the alkaloids retained by the sorbent were eluted using the mobile phase when the six-way valve was at the "Inject" position. The eluents for *C. roseus* and mouse plasma were 1.5 mL of MeOH-water (20:80, *V/V*) and 5 mL of water, respectively. In terms of the mobile phase, MeOH-ACN-water (0.2% triethylamine) (46:12:42, *V/V/V*) was used for isolating vinca alkaloids from *C. roseus* and ACN-water (42:58, *V/V*) for *Uncaria* alkaloids from mouse plasma.

## 3. Results and discussion

### 3.1. Synthesis of TpTph-MA-COF

The morphology of the TpTph-MA-COF, as characterized by SEM, is shown in Fig. 1A. The morphology exhibits an edge-curled petal-like structure. It is worth noting that the crimped edges of the petals have a supporting function that can hinder the face-to-face contact of different structural units, which can protect the microporous structure and maintain the high specific surface area and rich COF interaction sites. Furthermore, this dominant characteristic is more meaningful in the following step of preparing the POPM/COF to prevent the micropores from being masked by the accumulated polymer particle. The IR spectra shown in Fig. 1B indicate the successful synthesis of the COF: the absorption peak at ~1576 $cm^{-1}$ is attributed to $\nu_{C=N}$. The peaks that should be present at ~1725 $cm^{-1}$ ($\nu_{C=O}$ of aldehyde group), ~2820 $cm^{-1}$ and ~2720 $cm^{-1}$ ($\nu_{C-H}$ of aldehyde group), as well as ~3500 $cm^{-1}$ and ~3400 $cm^{-1}$ ($\nu_{NH}$ of primary amine group), are absent, which can be explained by the successful Schiff-base reaction. Furthermore, the peaks at ~1616 $cm^{-1}$ ($\nu_{C=O}$) and ~1288 $cm^{-1}$ ($\nu_{C-O-C}$) are produced by the ester group of MA, and the redshift of $\nu_{C=O}$ is deduced by the large conjugate of the COF. The powder X-ray diffraction (PXRD) image in Fig. 1C further confirms the good ordering of TpTph-MA-COF and shows an extremely high intensity peak at ~3.6° 2θ and low intensity peaks at ~7.31 and ~19–25° 2θ [41]. Fig. 1D is the nitrogen adsorption-desorption isotherm, which indicates a micro- and mesoporous structure with a *Brunauer–Emmett–Teller* (BET) surface area of 679.47 $m^2/g$.

### 3.2. Preparation of POPM/COF sorbents

In terms of sorbent A, the effects of the monomer/crosslinker (DAM/EDMA) ratio and porogens on the permeability of the prepared sorbents were investigated. The results are shown in Table 1 and indicate that increasing the crosslinker/monomer ratio resulted in low permeability (sorbents A1–A3). Although high permeability is a desired property for SPE sorbents, this is usually accompanied by relatively poor mechanical stability, so sorbent A2 with a monomer/crosslinker ratio of 0.4/0.45 (*V/V*) exhibiting moderate permeability and proper mechanical stability was adopted for further investigation. TpTph-MA-COF plays an important role in the preparation of composite POPM/COF, as the properties of sorbents A2 and A4–A6 demonstrate. TpTph-MA-COF has a large specific surface area and a curly petal-like structure, which can effectively enhance the surface area of the resulting composite

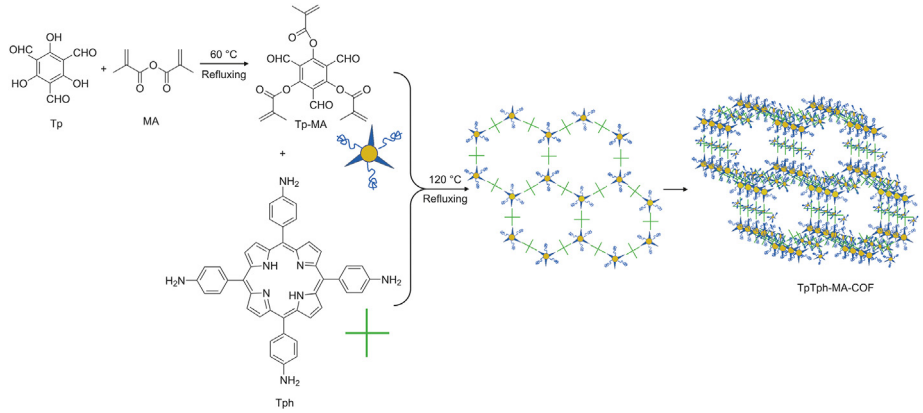


**Scheme 1.** Synthesis route of TpTph-MA-COF.

**Table 1**
Representative composition of the pre-polymerization solution and resulting properties of the POPM/COF sorbents.

| Sorbent [a] | Crosslinker (mL) | | Porogen (mL) | | | COF (mg) | Back pressure [b] ($10^5$ Pa) | Permeability [c] ($K$, $10^{-14}$ $m^2$) | BET surface area ($m^2$/g) |
|---|---|---|---|---|---|---|---|---|---|
| | EDMA | TAIC | n-propyl alcohol | Dodecanol | DMF | | | | |
| A1 | 0.35 | – | 0.3 | 0.6 | – | 5 | 14 | 2.08 | 151.73 |
| A2 | 0.45 | – | 0.3 | 0.6 | – | 5 | 18 | 1.62 | 153.14 |
| A3 | 0.55 | – | 0.3 | 0.6 | – | 5 | >2 | <1.42 | 157.13 |
| A4 | 0.45 | – | 0.3 | 0.6 | – | 2 | 7 | 4.15 | 141.54 |
| A5 | 0.45 | – | 0.3 | 0.6 | – | 10 | >26 | <1.12 | 173.19 |
| A6 | 0.45 | – | 0.3 | 0.6 | – | 0 | 5 | 5.82 | 76.33 |
| B1 | 0.45 | 0.45 | 0.7 | 1.0 | 0.2 | 5 | 5 | 5.82 | 76.41 |
| B2 | 0.45 | 0.45 | 0.7 | 1.0 | 0.2 | 10 | 6 | 4.85 | 78.32 |
| B3 | 0.45 | 0.45 | 0.7 | 1.0 | 0.2 | 15 | 9 | 3.23 | 80.01 |
| B4 | 0.45 | 0.45 | 0.7 | 1.0 | 0.2 | – | 5 | 5.82 | 33.25 |

[a] Sorbents A were prepared using DAM (0.4 mL) as the monomer, and initiated by BPO/DMA (0.01 g/50 μL); Sorbents B were prepared using THFMA (0.2 mL) as the monomer, and initiated by BPO/DMA (0.01 g/30 μL).
[b] MeOH was used as the mobile phases with a flow rate of 1.0 mL/min.
[c] Permeability was calculated following Darcy's law using MeOH (the viscosity is 0.58 × $10^{-3}$ Pa·s at 25 °C) as the mobile phase.

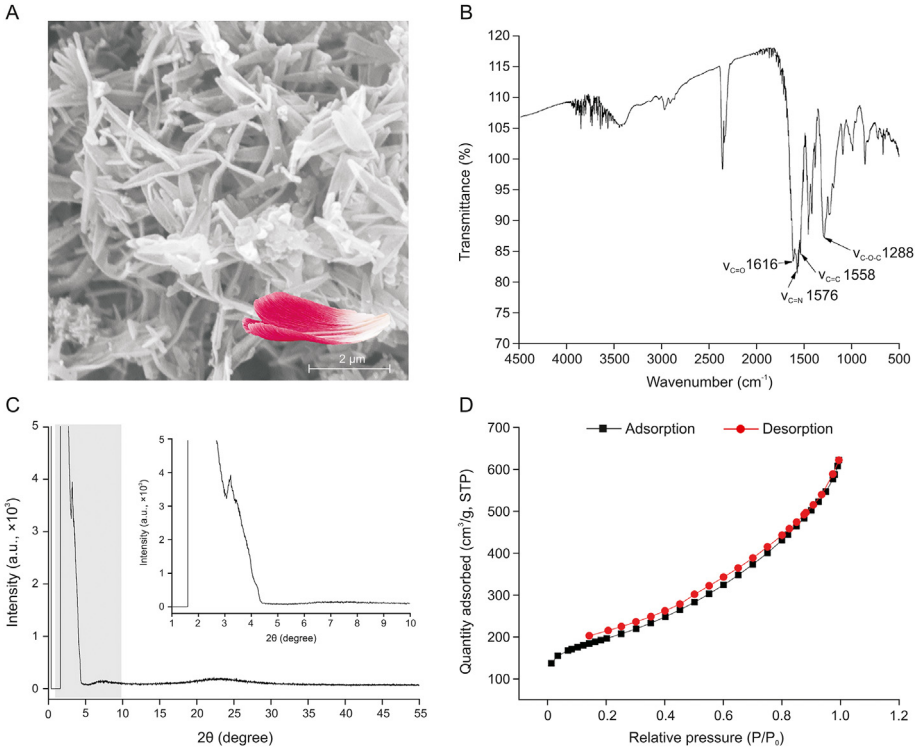


**Fig. 1.** (A) Petal-like scanning electron microscope image, (B) IR spectra, (C) powder X-ray diffraction pattern, and (D) adsorption-desorption isotherm of TpTph-MA-COF.

POPM/COF, and this conclusion can be confirmed by the BET surface area of sorbents A1–A6 and B1–B4 shown in Table 1. Given the same conditions, a higher COF ratio in the pre-polymerization solution results in a larger composite POPM/COF sorbent area. Concurrently, a high COF ratio will lead to a low permeability. Thus, 5 and 15 mg of added COF resulted in proper permeability and were selected for preparing sorbents A and B.

The mass of prepared sorbent A was 0.1104 g and sorbent B was 0.1208 g, and the rod-shaped sorbent sizes were both 50 mm × 4.6 mm, as defined by the stainless steel tube.

The SEM images shown in Fig. 2 indicate the morphologies of the resulting composite POPM/COF sorbents. This result confirms that the macroporous structure of the POPMs is not disturbed by introducing TpTph-MA-COF. Although the micropore structure of TpTph-MA-COF cannot be seen in the SEM images because of its microsize, the IR spectra shown in Supplementary data and Fig. S4 confirm the successful fabrication of the composite POPM/COF. Furthermore, the porous structure of each sorbent is consistent with its corresponding permeability.

The pore size distribution and specific surface area of the composite POPM/COF sorbents were measured using the nitrogen adsorption-desorption method, and the adsorption-desorption isotherms are shown in Supplementary data and Fig. S5. Furthermore, the detailed pore-size data of the optimized sorbents A2 and B3 are shown in Supplementary data and Fig. S6 and indicate the micro- and mesopore size distributions of the sorbents. The micropores are produced by the COF units, and the mesopores are deduced by the gaps in the accumulations of the composite

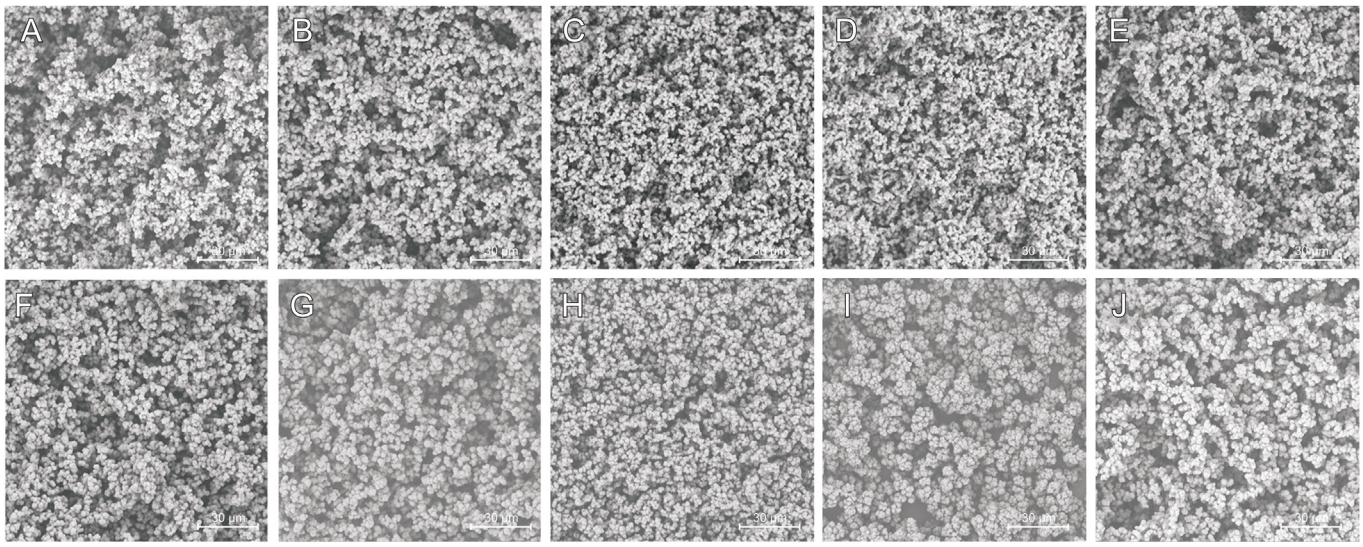


**Fig. 2.** SEM images of sorbents A and B. Sorbents A1–A6 are successively marked as A–F, and B1–B4 marked as G–J.

polymer particles. Considering the total properties, sorbents A2 and B3 had specific surface areas of 153.14 and 80.01 $m^2/g$, respectively, and were adopted as the best sorbents for further testing.

Furthermore, these results show that sorbents A and B both have pores with multiple macro-, meso-, and micropores, as well as multiple functional groups, which exhibit both high permeability and enhanced specific surface area and, thus, enrich the adsorption mode and adsorption amount for the target components.

### 3.3. Selectivity of the sorbents

Sorbent A, which contained carbonyl, ester and porphyrin groups (obtained from the monomer, crosslinker and COF), was used to extract vindoline, catharanthine and vincristine from the crude extraction of *C. roseus* via the interactions of dipole-dipole, hydrogen bond, π-π, etc. The vinca alkaloids occupying the benzene ring have π-π interaction with porphyrin groups of sorbent A. Furthermore, the hydroxyl groups of vindoline and vincristine with strong polarity show hydrogen bond interaction with carbonyl and ether groups of sorbent A. Furthermore, hydrophobic interaction between vinca alkaloids and sorbent A is also a main role. These interactions result in the behavior of vinca alkaloids on sorbent A. Multiple components are contained in the crude extraction solution of *C. roseus*, which not only disturbs the quantitative analysis of the target alkaloids but also blocks the analytical column. As a result, an eluent used in the SPE procedure should have proper elution strength to remove the matrices and simultaneously retain the alkaloids. According to the results of investigations shown in Fig. S7, 1.5 mL of MeOH-water (20:80, *V/V*) exhibiting proper elution strength was used as the eluent. As shown in Fig. S8, the alkaloids could be retained by sorbent A when the MeOH-water (20:80, *V/V*) eluent was used and could then be eluted when MeOH-ACN-water (0.2% triethylamine) (46:12:42, *V/V/V*) was used as the mobile phase. These results show that sorbent A can simultaneously remove part of the matrices of the crude extraction and selectively extract these three alkaloids with high efficiency.

Sorbent B, which has four hydrogen furfuryl, carbonyl, tertiary amine and porphyrin groups, will undergo dipole-dipole, hydrogen bond, π-π, etc., interactions with the isocorynoxeine, isorhynchophylline, corynoxeine and rhynchophylline alkaloids. The large conjugated structure provided by the porphyrin groups of sorbent B interacts with the benzene ring structure of *Uncaria* alkaloids, as well as the four-hydrogen furfuryl and ester groups in the sorbent produce hydrogen bond interaction with *Uncaria* alkaloids. The results shown in Supplementary data and Fig. S9 indicate that the matrices of the mouse plasma can be almost totally removed using water as the eluent, and the four alkaloids can be eluted using ACN-water (42:58, *V/V*) as the mobile phase followed by selective adsorption by sorbent B. These results confirm that sorbent B can be used to pre-treat mouse plasma containing isocorynoxeine, isorhynchophylline, corynoxeine and rhynchophylline.

The main mechanism of matrix removal is size exclusion based on the molecular kinetic diameters: the protein and polysaccharide macromolecules with complex and three-dimensional structures cannot easily pass through the meso- and micropores, while these molecules can easily pass through the macropores that have a

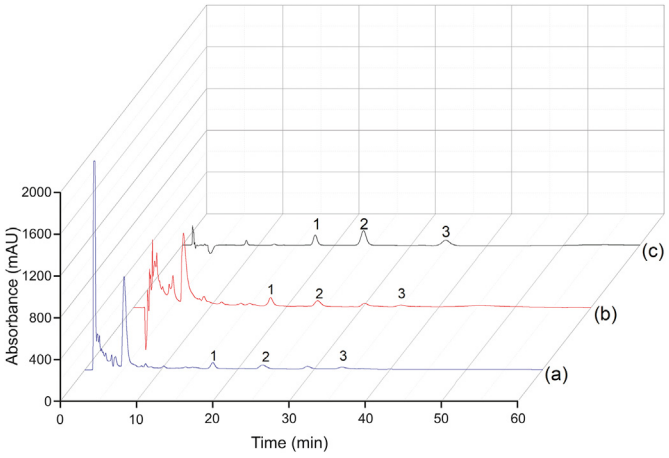


**Fig. 3.** Effect of *C. roseus* matrix. Chromatograms of *C. roseus* extract solution before the SPE procedure (a), after the SPE procedure (b) and the standard solution after the SPE procedure (c). Conditions: Sorbent A (50 mm × 4.6 mm) and the HPLC system were combined using a ZORBAX Eclipse Plus $C_{18}$ column (150 mm × 4.6 mm i.d., 5 μm), the flow rate was 1.0 mL/min, the wavelength was 220 nm, the samples were crude extract solution of *C. roseus* and the reference standard alkaloid solution (0.1 mg/mL), the injection volume was 5 μL, the eluent was 1.5 mL of MeOH-water (20:80, *V/V*), and the mobile phase was MeOH-ACN-water (0.2% triethylamine) (46:12:42, *V/V/V*). 1: vindoline; 2: catharanthine; 3: vincristine.

relatively low coverage of chemical groups and, thus, are not retained. Small alkaloid molecules can easily pass through the meso- and micropores with relatively high functional group coverage. Thus, the alkaloid molecules will be selectively retained by many interaction sites. Compared to conventional restricted access matrix sorbents [42,43], the pore structure of the POPM/COF sorbents can be easily controlled, and multifunctional groups are flexibly grafted. Molecules with different dynamic diameters will pass through the compatible pores: biological macromolecules, such as proteins with three-dimensional structures, will pass through the macropores, whose surface has been grafted with the porphyrin-based COF units, and the porphyrin-based COF, which has good biocompatibility with the proteins, can avoid denaturing and the precipitating adsorption of the proteins. Regardless of whether the target small molecules pass through the macro-, meso- or micropores, these targets can be retained with the rich interaction sites on the sorbent surface through multiple mechanisms, thus avoiding loss.

### 3.4. Applicability

This experiment is in full compliance with the Animal Management Regulations, National Science and Technology Commission, China, and was approved by the Institutional Ethics Committee of Hebei University. Crude extraction solutions of *C. roseus* and the vindoline, catharanthine and vincristine reference standard solutions were used as the applicable test samples for sorbent A, and the results are shown in Fig. 3. Compared to the chromatogram in Fig. 3a (obtained before the SPE with the optimized chromatographic condition), there is a relatively low peak from the matrices before 10 min in the chromatogram in Fig. 3b (obtained after SPE). This result indicates that the matrices of the crude *C. roseus* extraction have been mostly removed, and the height of the peaks for the target alkaloids has been enhanced. Fig. 3c is the chromatogram of the reference standard alkaloids and confirms the retention time of the three alkaloids. These results indicate that sorbent A combined with an HPLC system using a $C_{18}$ column can be used for the online extraction and analysis of the three alkaloids in *C. roseus*. Concurrently, spiked plasma with isocorynoxeine, isorhynchophylline, corynoxeine and rhynchophylline reference standards was used as the sample for testing sorbent B, and the results are shown in Fig. 4. The large peak found at the dead time in the chromatogram of Fig. 4a (obtained before the SPE with the optimized chromatographic condition) is the plasma proteins, which easily produce irreversible adsorption on the $C_{18}$ column. Fig. 4b is the chromatogram obtained after SPE, indicating that the plasma proteins have been removed and that the four target peaks are not affected. Fig. 4c is the chromatogram of blank plasma obtained using the SPE-HPLC procedure, indicating that there is no endogenous substance that interferes with the target peaks. These results indicate that sorbent B combined with an HPLC system using a $C_{18}$ column can be used for the online extraction and analysis of the four alkaloids in mouse plasma.

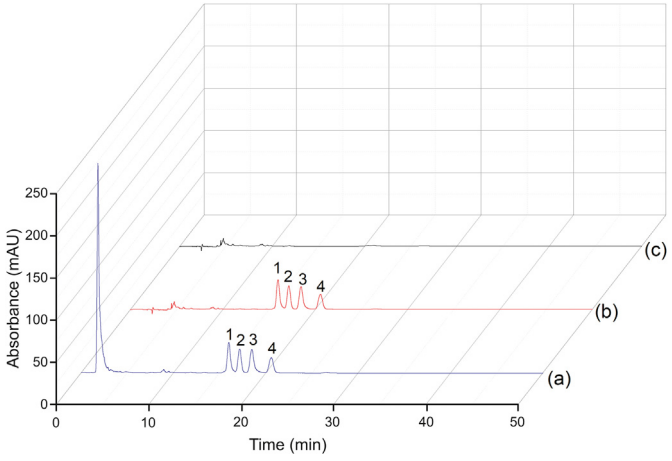


**Fig. 4.** Effect of the mouse plasma matrix. Chromatograms of *Uncaria* alkaloid-spiked rat plasma before the SPE procedure (a), after the SPE procedure (b) and blank plasma after the SPE procedure (c). Conditions: Sorbent B (50 mm × 4.6 mm) and the HPLC system were combined using a COSMOSIL C18 column (250 mm × 4.6 mm i.d., 5 μm), the flow rate was 1.0 mL/min, the wavelength was 254 nm, the samples were blank plasma and alkaloid spiked plasma (0.02 mg/mL), the injection volume was 10 μL, the eluent was 5 mL of water, and the mobile phase was ACN-water (42:58, *V/V*). 1: isocorynoxeine; 2: isorhynchophylline; 3: corynoxeine; 4: rhynchophylline.

### 3.5. Enrichment and adsorption capacity

Crude extractions of alkaloids from *C. roseus* and *Uncaria* were enriched using sorbents A and B, respectively, to investigate the enrichment capacity of the two sorbents. As shown in Fig. S10a, the peak areas of vindoline, catharanthine and vincristine are proportional to the injection volume, and there is no interference disturbing the target peaks, thus indicating the good enrichment capacity of sorbent A. In Fig. S10b, the peak areas of isocorynoxeine, isorhynchophylline, corynoxeine and rhynchophylline are proportional to the injection volume, and there is no interference disturbing the target peaks, thus indicating the good enrichment capacity of sorbent B. These results show that the composite POPM/COF sorbents have not only excellent adsorption ability but also specific selectivity for the target indole alkaloids due to the multiple recognition sites obtained from the multifunctional chemical groups on the sorbents with multisize pores.

The adsorption capacity of sorbent A for the representative catharanthine alkaloid is 14.26 mg/g, and the adsorption capacity of sorbent B for rhyncholphylline is 11.59 mg/g, with the adsorption curves shown in Fig. S11. However, the adsorption capacity of sorbents A6 and B4 that without COF is 3.31 mg/g and 4.79 mg/g, using catharanthine and rhyncholphylline as the test sample, respectively. Compared to the adsorption capacity of 14.26 mg/g and 11.59 mg/g, the lower adsorption capacity results can be explained by the smaller specific surface area of the sorbents. In other words, the adsorption capacity of the sorbent can be increased by adding COF to increase the specific surface area.

### 3.6. Method validation

The linearity, limits of detection (LODs), limits of quantitation (LOQs) and linear range are shown in Table S1. These results indicate the feasibility of the present method. The LODs (S/N=3/1) of vindoline, catharanthine and vincristine are in the range of 0.2–0.6 μg/mL, and the LOQs (S/N=10/1) are in the range of 0.5–1.5 μg/mL. The LODs (S/N=3/1) of isocorynoxeine, isorhynchophylline, corynoxeine and rhynchophylline are in the range of 3.5–4.6 ng/mL, and the LOQs (S/N=10/1) are in the range of 12–15 ng/mL. The $t$ values ($n$=8) for the regression equation intercepts of vindoline, catharanthine and vincristine obtained from the $t$ tests are 1.697, 0.928 and 2.437, respectively, which are lower than the theoretical $t$ values of 2.447 for 95% confidence levels ($n$=8); concurrently, the $t$ values ($n$=6) of isocorynoxeine, isorhynchophylline, corynoxeine and rhynchophylline are 1.250, 1.185, 1.198, and 1.121, respectively, which are lower than the theoretical $t$ values of 2.776 for 95% confidence levels ($n$=6). The detailed results of the $t$ tests are shown in Tables S2 and S3. The preparative repeatability of sorbents A and B was evaluated by pre-treating the

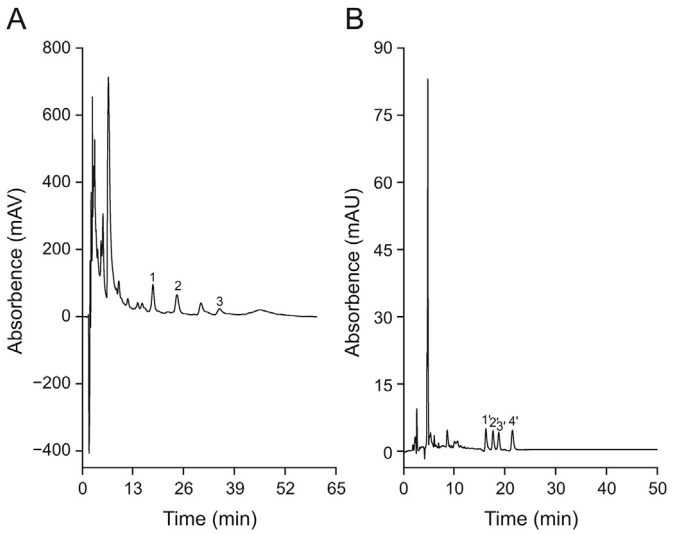


**Fig. 5.** Determination of the alkaloids in (A) real *C. roseus* extract and (B) mouse plasma samples. Conditions for (A) were the same as those of Fig. 3b except for an injection volume of 20 μL; conditions for (B): a mouse (20 g in weight) received 50 μL of *Uncaria* extract (decocted with water) by intragastric administration, and blood was sampled after 1 h and was subsequently pre-treated following the given procedure. The other corresponding conditions were the same as those in Fig. 4b. 1: vindoline; 2: catharanthine; 3: vincristine; 1': isocorynoxeine; 2': isorhynchophylline; 3': corynoxeine; 4': rhynchophylline.

corresponding alkaloids with six sorbents that were prepared separately. The relative standard deviations (RSDs, $n$=6) were found to be in the range of 0.48%–4.24% for peak area and 1.26%–1.69% for the retention time, thus indicating good preparative repeatability. The RSD values ($n$=6) of the method repeatability were in the range of 0.15%–0.90% (based on retention time) and 1.13%–3.46% (based peak area), which indicates the good repeatability of the method. The detailed data are shown in Table S4. The accuracy expressed by the spiked recovery is shown in Table S5 and Table S6, and recoveries in the ranges of 99.38%–100.91% and 96.39%–103.50% were obtained for vinca and *Uncaria* alkaloids, respectively.

The real samples, including crude extraction of *C. roseus* and mouse plasma (blood obtained from a mouse that had received the *Uncaria* extract with intragastric administration 1 h later), were quantitatively determined using the online SPE-HPLC system based on sorbent A-$C_{18}$ and sorbent B–$C_{18}$, respectively, and the chromatograms are shown in Fig. 5. The vindoline, catharanthine and vincristine contents in *C. roseus* were 0.70, 0.28, and 0.28 mg/g, respectively, and the isocorynoxeine, isorhynchophylline, corynoxeine and rhynchophylline contents were 10.54, 11.22, 8.20, and 9.76 μg/g, respectively.

Sorbents A and B that were used as the SPE columns were injected more than 100 times, and the RSD values based on the peak areas of vinca alkaloids and *Uncaria* alkaloids were ≤5.32% (n ≥ 100) and ≤ 4.87% (n ≥ 100), respectively. These results indicate the good reusability of the present SPE sorbents.

### 3.7. Advantages of the present method

In terms of pre-treating alkaloids in complex samples, compared to other reported studies [44–48], the present work showed the advantage of wide application and can be applied for not only plant extraction but also blood samples. Furthermore, the present work shows better linearity with a coefficient of determination ($R^2$) > 0.9979 [44,45] and better recovery (99.38%–100.91%; 96.39%–103.50%) [44–47]. Compared to reference methods [47,48], the proposed method based on POPM/COF showed lower LODs and LOQs. Furthermore, it is worth noting that the POPM/COF-SPE sorbents exhibit strong reusability, being used more than 100 times. These comparisons confirm that the present work is a simple and efficient method for the extraction and concentration of alkaloids in complex biological samples. The detailed comparable data with other reported studies are shown in Table S7.

## 4. Conclusions

The present work has established a facile on-line extraction and quantitative analytical method by fabricating multifunction sorbents with multisize pores with the goal of addressing problems presented in the analysis of complex biological samples. Although porous organic polymer materials have exhibited an outstanding applicability in the separation and adsorption fields, promising prospects are limited by the disadvantage of low surface area. In this study, a functional porphyrin-based COF was synthesized and introduced to porous organic polymer materials via a polymerization reaction using grafted double bonds, combining the advantages of the high specific surface area and macroporous structure of the two material types. Furthermore, the “edge-curled petal-like” features of the obtained COF are significant for the preparation of the composite POPM/COF. These features supplied stereo space and prevented the micropores from being filled by the polymer particles. The COF based on porphyrin units and grafted onto the POPM/COF sorbent has played an important role in removing biological matrices while not denaturing proteins due to its specific biocompatibility with the primary proteins contained in the sample matrix. As a result, the fabricated composite POPM/COF materials exhibit a macroporous structure with an enhanced specific surface area and show excellent clean-up ability with respect to the matrices of crudely extracted medicinal plants and mouse plasma. This is achieved through size exclusion and concurrently exhibiting good specific selectivity for the alkaloids according to the multiple interaction sites covering the surface of the sorbent. Moreover, multiple composite materials can be prepared following the present method, and these materials can target different trace or micro concentration components in complex biological samples. This ability highlights the value of the preparative method.

## CRediT author statement

**Fanrong Sun:** Methodology, Validation, Writing - Original draft preparation; **Ligai Bai:** Conceptualization, Writing - Reviewing and Editing, Funding acquisition; **Mingxue Li:** Investigation, Data curation; **Changqing Yu:** Investigation; **Haiyan Liu:** Funding acquisition; **Xiaoqiang Qiao:** Data curation; **Hongyuan Yan:** Supervision.

## Declaration of competing interest

The authors declare that there are no conflicts of interests.

## Acknowledgments

This work was supported by the Natural Science Foundation of Hebei Province (Grant No.: B2020201002), the National Natural Science Foundation of China (Grant Nos.: 21974034 and 21505030), and the Interdisciplinary Research Project of Natural Science of Hebei University (Grant No.: DXK201912).

## Appendix A. Supplementary data

Supplementary data to this article can be found online at https://doi.org/10.1016/j.jpha.2020.12.006.

## References


[1] X. Guan, F. Chen, Q. Fang, et al., Design and applications of three dimensional covalent organic frameworks, Chem. Soc. Rev. 49 (2020) 1357–1384.
[2] F. Yuan, J. Tan, J. Guo, Assemblies of covalent organic framework microcrystals: multiple-dimensional manipulation for enhanced applications, Sci. China Chem. 61 (2018) 143–152.
[3] G. Liu, J. Sheng, Y. Zhao, Chiral covalent organic frameworks for asymmetric catalysis and chiral separation, Sci. China Chem. 60 (2017) 1015–1022.
[4] M.S. Lohse, T. Bein, Covalent organic frameworks: structures, synthesis, and applications, Adv. Funct. Mater. 28 (2018), 1705553.
[5] J.L. Segura, M.J. Mancheño, F. Zamora, Covalent organic frameworks based on Schiff-base chemistry: synthesis, properties and potential applications, Chem. Soc. Rev. 45 (2016) 5635–5671.
[6] Y. Hu, N. Goodeal, Y. Chen, et al., Probing the chemical structure of monolayer covalent-organic frameworks grown via Schiff-base condensation reactions, Chem. Commun. (Camb) 52 (2016) 9941–9944.
[7] S. Zhuang, R. Chen, Y. Liu, et al., Magnetic COFs for the adsorptive removal of diclofenac and sulfamethazine from aqueous solution: adsorption kinetics, isotherms study and DFT calculation, J. Hazard Mater. 385 (2020), 121596.
[8] C. Liu, E. Park, Y. Jin, et al., Separation of arylenevinylene macrocycles with a surface confined two-dimensional imine covalent organic framework, Angew. Chem. Int. Ed. Engl. 57 (2018) 8984–8988.
[9] H.-L. Qian, C.-X. Yang, W.-L. Wang, et al., Advances in covalent organic frameworks in separation science, J. Chromatogr. A 1542 (2018) 1–18.
[10] J.-M. Liu, X.-Z. Wang, C.-Y. Zhao, et al., Fabrication of porous covalent organic frameworks as selective and advanced adsorbents for the on-line preconcentration of trace elements against the complex sample matrix, J. Hazard Mater. 344 (2018) 220–229.
[11] K. Dey, H.S. Kunjattu, A.M. Chahande, et al., Nanoparticle size-fractionation through self-standing porous covalent organic framework films, Angew. Chem. Int. Ed. Engl. 59 (2020) 1161–1165.
[12] Y. Li, X. Guo, X. Li, et al., Redox-active two-dimensional covalent organic frameworks (COFs) for selective reductive separation of valence-variable, redox-sensitive and long-lived radionuclides, Angew. Chem. Int. Ed. Engl. 59 (2020) 4168–4175.
[13] X. Ding, J. Yang, Y. Dong, Advancements in the preparation of high-performance liquid chromatographic organic polymer monoliths for the separation of small-molecule drugs, J. Pharm. Anal. 8 (2018) 75–85.
[14] S. Eeltink, S. Wouters, J.L. Dores-Sousa, et al., Advances in organic polymer-based monolithic column technology for high-resolution liquid chromatography-mass spectrometry profiling of antibodies, intact proteins, oligonucleotides, and peptides, J. Chromatogr. A 1498 (2017) 8–21.
[15] D. Xu, E. Sánchez-López, Q. Wang, et al., Determination of L-norvaline and L-tryptophan in dietary supplements by nano-LC using an O-[2-(meth-acryloyloxy)-ethylcarbamoyl]-10,11-dihydroquinidine-silica hybrid monolithic column, J. Pharm. Anal. 10 (2020) 70–77.
[16] Z. Liu, J. Ou, H. Lin, et al., Preparation of monolithic polymer columns with homogeneous structure via photoinitiated thiol-yne click polymerization and their application in separation of small molecules, Anal. Chem. 86 (2014) 12334–12340.
[17] R. Poupart, D. Grande, B. Carbonnier, et al., Porous polymers and metallic nanoparticles: a hybrid wedding as a robust method toward efficient supported catalytic systems, Prog. Polym. Sci. 96 (2019) 21–42.
[18] Y. Chen, L. Xia, R. Liang, et al., Advanced materials for sample preparation in recent decade, Trac. Trends Anal. Chem. 120 (2019), 115652.
[19] H. Liu, H. Yu, P. Jin, et al., Preparation of mesoporous silica materials functionalized with various amino-ligands and investigation of adsorption performances on aromatic acids, Chem. Eng. J. 379 (2020), 122405.
[20] W.-J. Zhang, D. Li, Y. Xu, et al., Synthesis and application of novel molecularly imprinted solid phase extraction materials based on carbon nanotubes for determination of carbofuran in human serum by high performance liquid chromatography, J. Agric. Food Chem. 67 (2019) 5105–5112.
[21] Y. Han, Z. Wang, J. Jia, et al., Newly designed molecularly imprinted 3-aminophenol-glyoxal-urea resin as hydrophilic solid-phase extraction sorbent for specific simultaneous determination of three plant growth regulators in green bell peppers, Food Chem. 311 (2020), 125999.
[22] I. Mohiuddin, A. Grover, J.S. Aulakh, et al., Porous molecularly-imprinted polymer for detecting diclofenac in aqueous pharmaceutical compounds, Chem. Eng. J. 382 (2020), 123002.
[23] S. Tang, H. Zhang, H.K. Lee, Advances in sample extraction, Anal. Chem. 88 (2015) 228–249.
[24] C. Herrero-Latorre, J. Barciela-García, S. García-Martín, et al., Graphene and carbon nanotubes as solid phase extraction sorbents for the speciation of chromium: a review, Anal. Chim. Acta 1002 (2018) 1–17.
[25] M. Manouchehri, S. Seidi, A. Rouhollahi, et al., Micro solid phase extraction of parabens from breast milk samples using Mg-Al layered double hydroxide functionalized partially reduced graphene oxide nanocomposite, Food Chem. 314 (2020), 126223.
[26] K. Jiang, Q. Huang, K. Fan, et al., Reduced graphene oxide and gold nanoparticle composite-based solid-phase extraction coupled with ultra-high-performance liquid chromatography-tandem mass spectrometry for the determination of 9 mycotoxins in milk, Food Chem. 264 (2018) 218–225.
[27] L. Li, Y. Chen, L. Yang, et al., Recent advances in applications of metal–organic frameworks for sample preparation in pharmaceutical analysis, Coord. Chem. Rev. 411 (2020), 213235.
[28] Y. Hara, K. Kanamori, K. Nakanishi, Self-assembly of metal-organic frameworks into monolithic materials with highly controlled trimodal pore structures, Angew. Chem. 131 (2019) 19223–19229.
[29] L.G. Christie, Captivating COFs, Nat. Chem. 8 (2016), 406.
[30] E.V.S. Maciel, A.L. de Toffoli, E.S. Neto, et al., New materials in sample preparation: recent advances and future trends, Trac. Trends Anal. Chem. 119 (2019), 115633.
[31] B. Hashemi, P. Zohrabi, M. Shamsipur, Recent developments and applications of different sorbents for SPE and SPME from biological samples, Talanta 187 (2018) 337–347.
[32] L. Xia, J. Yang, R. Su, et al., Recent progress in fast sample preparation techniques, Anal. Chem. 92 (2020) 34–48.
[33] T. Zhou, G. Che, L. Ding, et al., Recent progress of selective adsorbents: from preparation to complex sample pretreatment, Trac. Trends Anal. Chem. 121 (2019), 115678.
[34] J. Yan, J. Ding, G. Jin, et al., Profiling of sialylated oligosaccharides in mammalian milk using online solid phase extraction-hydrophilic interaction chromatography coupled with negative-ion electrospray mass spectrometry, Anal. Chem. 90 (2018) 3174–3182.
[35] L.C. da Silva, M.C. Souza, B.R. Sumere, et al., Simultaneous extraction and separation of bioactive compounds from apple pomace using pressurized liquids coupled on-line with solid-phase extraction, Food Chem. 318 (2020), 126450.
[36] E. Milanetti, G. Carlucci, P.P. Olimpieri, et al., Correlation analysis based on the hydropathy properties of non-steroidal anti-inflammatory drugs in solid-phase extraction (SPE) and reversed-phase high performance liquid chromatography (HPLC) with photodiode array detection and their applications to biological samples, J. Chromatogr. A 1605 (2019), 360351.
[37] J. Marín-Sáez, R. Romero-González, A. Garrido Frenich, Reliable determination of tropane alkaloids in cereal based baby foods coupling on-line SPE to mass spectrometry avoiding chromatographic step, Food Chem. 275 (2019) 746–753.
[38] L.-H. Liu, C.-X. Yang, X.-P. Yan, Methacrylate-bonded covalent-organic framework monolithic columns for high performance liquid chromatography, J. Chromatogr. A 1479 (2017) 137–144.
[39] G. Lin, H. Ding, R. Chen, et al., 3D porphyrin-based covalent organic frameworks, J. Am. Chem. Soc. 139 (2017) 8705–8709.
[40] R. Chen, J.-L. Shi, Y. Ma, et al., Designed synthesis of a 2D porphyrin-based $sp^2$ carbon-conjugated covalent organic framework for heterogeneous photocatalysis, Angew. Chem. Int. Ed. Engl. 58 (2019) 6430–6434.
[41] D.B. Shinde, S. Kandambeth, P. Pachfule, et al., Bifunctional covalent organic frameworks with two dimensional organocatalytic micropores, Chem. Commun. (Camb) 51 (2015) 310–313.
[42] R.K. Sharma, P. Yadav, M. Yadav, et al., Recent development of covalent organic frameworks (COFs): synthesis and catalytic (organic-electro-photo) applications, Mater. Horiz. 7 (2020) 411–454.
[43] F.A.C. Suquila, L.L.G. de Oliveira, C.R.T. Tarley, Restricted access copper imprinted poly(allylthiourea): the role of hydroxyethyl methacrylate (HEMA) and bovine serum albumin (BSA) on the sorptive performance of imprinted polymer, Chem. Eng. J. 350 (2018) 714–728.
[44] R. Chen, Z. Ning, C. Zheng, et al., Simultaneous determination of 16 alkaloids in blood by ultrahigh-performance liquid chromatography-tandem mass spectrometry coupled with supported liquid extraction, J. Chromatogr. B Analyt. Technol. Biomed. Life Sci. 1128 (2019), 121789.
[45] K. Hu, T. Pang, Y. Shi, et al., Facile preparation of a magnetic porous organic frameworks for highly sensitive determination of eight alkaloids in urine samples based UHPLC-MS/MS, Microchem. J. 157 (2020), 105048.
[46] C.-W. Chang, Y.-Y. Yeh, L.-C. Chang, et al., Rapid determination of oxindole alkaloids in Cat's claw by HPLC using ionic liquid-based microwave-assisted extraction and silica monolithic column, Biomed. Chromatogr. 31 (2017), e3925.
[47] D.F. Rambo, R. Biegelmeyer, N.S.B. Toson, et al., Box–Behnken experimental design for extraction optimization of alkaloids from *Erythrina verna* Vell. trunk barks and LC Method Validation, Ind. Crops Prod. 133 (2019) 250–258.
[48] Y. Liu, D. Xie, Y. Kang, et al., Microwave-assisted extraction followed by solid-phase extraction for the chromatographic analysis of alkaloids in *Stephania cepharantha*, J. Chromatogr. Sci. 54 (2016) 670–676.